Breakdown of the bounding properties of variational transition state theory and the Rayleigh quotient method

Alexander N. Drozdov* and Susan C. Tucker
Department of Chemistry, University of California, Davis, California 95616
(Received 1 November 1999)

The thermally activated escape of a Brownian particle from one metastable state to another by crossing an intervening potential barrier is studied by means of variational transition state theory (VTST) and a Rayleigh quotient method. Historically, these two methods have been shown to provide an upper bound to the ''rate constant,'' and a restricted identity between them has been recently demonstrated by Talkner and Pollak [Phys. Rev. E **50**, 2646 (1994)]. Yet, we show that while VTST gives an upper bound to a specific definition of the ''reactive flux rate,'' neither VTST nor this reactive flux rate provide a rigorous upper bound to the least nonvanishing eigenvalue of the underlying Fokker–Planck operator, as is done by the Rayleigh quotient method in the Smoluchowski limit. Numerical results for the rate in a symmetric double well show that in the spatial diffusion regime, the failure of the VTST and reactive flux methods is only significant for relatively low barriers, e.g., $\beta E \lesssim 5$.

PACS number(s): 05.40.−a, 82.20.Db, 82.20.Fd

I. INTRODUCTION

The Rayleigh–Ritz variational method is known to be a very powerful tool for systematically treating Sturm-Liouville problems of quantum mechanics and statistics [1]. The central advantage of this approach is that when applied to a Hermitian operator $\mathcal{H}$ it ensures the traditional upper bound property to the exact eigenvalues of this operator

$$\mathcal{E} \leqslant \frac{(\Psi, \mathcal{H}\Psi)}{(\Psi, \Psi)}, \tag{1.1}$$

with (f,g) denoting the scalar product. The latter property allows one to solve approximately the stationary Schrödinger equation by making use of a physically motivated trial ansatz for the wave function Ψ. The energy-expectation functional is varied with respect to free parameters entering the trial function to obtain the global minimum, which then provides the best approximation to the true eigenvalue. A similar approach is also available for efficiently solving the time-dependent Schrödinger equation [2]

$$i\hbar\dot{\Psi}(\mathbf{z},t) = \mathcal{H}\Psi(\mathbf{z},t), \tag{1.2}$$

where the dot denotes the time derivative. These methods are among the very few tools in the arsenal of quantum field theory and many-body theory, where alternative numerical techniques are expensive or unfeasible.

In contrast, nonequilibrium statistical mechanics is lacking a variational principle of the same flexibility as in quantum theory, capable of determining both the steady-state and the time-dependent solution to the initial-value problem. Although the Liouville equation for the probability density function in the nonequilibrium problems,

$$\dot{P}(\mathbf{z},t) = LP(\mathbf{z},t), \tag{1.3}$$

is analogous to the Schrödinger equation for the wave function, Eq. (1.2), there is a mathematical obstacle to applying the quantum variational principle to this analogous case. The obstacle arises because the evolution operator L is in general non-Hermitian for dissipative dynamical systems of interest. As will be described below, the modern theory of thermally activated rate processes [3–5], which is essentially due to Kramers [6], suffers from this problematic state of affairs.

Kramers [6] studied the motion of a Brownian particle with mass-weighted coordinate x, which can be thought to represent the reaction coordinate of a chemical reaction. The particle moves in a potential of mean force $U(x)$, such that it may switch from one metastable state A [i.e., the reactants $(x<0)$] to another state B [i.e., the products $(x>0)$] by crossing over a potential barrier at $x=0$ (see Fig. 1). The quantity of interest is then the escape rate Γ_A of the particle from the well, which corresponds to the chemical reaction rate. The energy required for this particle to cross the barrier must be supplied by the surrounding heat bath. In the Brownian approximation, the bath is assumed to have a vanishingly small correlation time such that a Markovian process results for the considered system. The time evolution of the corresponding probability density for this Brownian particle, $P(\mathbf{z},t)$, in phase space $\mathbf{z}=(x,v)$, is governed by the Fokker-Planck equation with the operator L given by

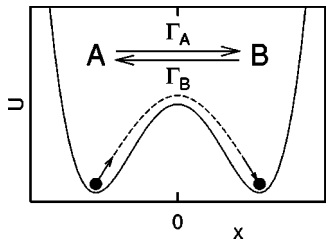

FIG. 1. Schematic graph of a two-state process in a bistable potential $U(x)$.

*Permanent address: Institute for High Temperatures, 13/19 Izhorskaya Street, 127412 Moscow, Russia.

$$L=-v\frac{\partial}{\partial x}+\frac{dU(x)}{dx}\frac{\partial}{\partial v}+\gamma\frac{\partial}{\partial v}\left(v+\beta^{-1}\frac{\partial}{\partial v}\right), \quad (1.4)$$

where γ is the friction coefficient, and β the inverse energy available from the thermal bath, $\beta^{-1}=k_BT$. One can easily check by substitution that the stationary (equilibrium) solution of the Fokker-Planck equation has the standard Maxwell–Boltzmann form

$$P_{eq}(x,v)=(\beta/2\pi)^{1/2}Z^{-1}\exp\{-\beta[\tfrac{1}{2}v^2+U(x)]\}, \quad (1.5)$$

$$Z=\int_{-\infty}^{\infty}dx\,\exp[-\beta U(x)].$$

The diffusion matrix associated with Eq. (1.4) does not possess an inverse, and, consequently, Eq. (1.4) cannot in principle be transformed to a Hermitian form. As a result, the powerful, nonperturbative schemes of quantum mechanics are generally inapplicable and cannot be used to solve the Kramers rate problem. However, in the strong friction limit ($\gamma\to\infty$), where the velocity relaxes to equilibrium infinitely rapidly and may therefore be eliminated adiabatically from the Fokker-Planck equation, Eqs. (1.3) and (1.4), this equation may be reduced to a Smoluchowski equation for the reduced probability

$$P(x,t)=\int_{-\infty}^{\infty}dv\,P(x,v,t) \quad (1.6)$$

with

$$L=\gamma^{-1}\frac{\partial}{\partial x}\left[\beta^{-1}\frac{\partial}{\partial x}+\frac{dU(x)}{dx}\right]. \quad (1.7)$$

Since the Smoluchowski operator is selfadjoint, variational methods of the standard form may be employed to obtain improved estimates for the escape rate Γ_A in this limiting case ($\gamma\to\infty$) [7,8]. The latter convenient fact is utilized in the Rayleigh quotient method [7–11], which recognizes that the least-nonvanishing eigenvalue of the underlying Fokker-Planck equation corresponds to the kinetic rate constant, i.e., the sum of the forward and backward escape rates, $\Gamma=\Gamma_A+\Gamma_B$. The general structure of this method is the same as in quantum mechanics [Eq. (1.1)] in that the least nonvanishing eigenvalue is calculated variationally from a trial eigenfunction. Typically, a physically motivated trial eigenfunction proposed by Kramers [6] is used. The principal advantages of the Rayleigh quotient method are that (i) it rigorously bounds the rate from above in the Smoluchowski ($\gamma\to\infty$) limit, and (ii) a first-order error in the trial function leads to only a second-order error in the estimate for the rate.

During the past two decades, a great deal of effort has been directed towards extending the applicability of such variational principles for the Fokker-Planck equation to the range of moderate friction. One popular strategy is based on the transformation of the original stochastic, dissipative system to an equivalent infinite dimensional Hamiltonian system [12]. Within the Hamiltonian formulation the escape rate Γ_A may be estimated, by means of transition state theory (TST), as a ratio of the equilibrium unidirectional flux through some chosen dividing surface to the population of the well [13–16]. The quality of such an estimate of the rate will, however, depend upon the choice of the dividing surface [13]. An attractive feature of this approach is that it is thought to give an upper bound to rate constants, such that a trial dividing surface may be varied to minimize the rate estimate [13,17–19], a procedure known as variational TST (VTST). Reviews of the present state of the art have recently been given by Tucker [20] and Pollak [21].

Although the Rayleigh quotient and VTST methods are very different, Talkner and Pollak [22] have recently demonstrated that there exists a restricted identity between them. Specifically, these authors were able to prove this identity in the case that VTST is limited to planar dividing surfaces and the Rayleigh quotient is limited to Kramers' trial functions. Since VTST has generally been thought to provide an upper bound to the true rate constant, Talkner and Pollak [22] concluded, quite reasonably, that their VTST–Rayleigh quotient identity proves the nontrivial result that the Rayleigh quotient method, when restricted to the class of Kramers functions, also bounds the rate from above for all values of the friction coefficient γ.

In this paper, we show that the identity between VTST and the Rayleigh quotient method breaks down for low barriers and that, as a result, Pollak and Talkner's conclusion about the bounding properties of the Rayleigh quotient is suspect in this limit. Perhaps more interestingly, we find that VTST itself does not provide a rigorous upper bound to the ''true'' rate constant, defined by the least nonvanishing eigenvalue of the Fokker–Planck operator, and may substantially underestimate it in the limit of low barriers. A striking consequence of this failure of VTST is that it implies a similar failure of the reactive flux method [as defined in Eq. (2.14)], since VTST *does* bound the reactive flux formula (based on the same dividing surface) from above. Comparison with exact numerical rates in a symmetric double well confirms these findings. The reminder of the paper is organized as follows. In Sec. II, a phenomenological rate law is reviewed, along with its connection to the reactive flux method, the TST rate, the Rayleigh quotient rate and the least nonzero eigenvalue of the Fokker–Planck operator. Disadvantages of the reactive flux method are discussed, and a way to improve it is suggested. Bounding properties are emphasized throughout. In Sec. III, we briefly outline and compare explicit expressions for the VTST and Rayleigh quotient methods. The bounding properties of these methods are then tested in Sec. IV by comparing analytical and numerical calculations of the rate in the limit of both strong and moderate friction. Section V concludes with some final remarks.

II. REACTIVE FLUX METHOD

To begin with, we review a phenomenological approach to the problem of interest and discuss its connection to the underlying dissipative dynamics, and, in particular, to the so-called ''reactive flux'' and to the least nonvanishing eigenvalue. The phenomenological approach is based on the assumption that the two-state process displayed in Fig. 1 can be described by a simple linear rate law [23,24]

$$\dot{\overline{N}}_A(t) = -\tilde{\Gamma}_A \overline{N}_A(t) + \tilde{\Gamma}_B \overline{N}_B(t),$$
$$\dot{\overline{N}}_B(t) = \tilde{\Gamma}_A \overline{N}_A(t) - \tilde{\Gamma}_B \overline{N}_B(t). \tag{2.1}$$

Here, $\tilde{\Gamma}_A$ and $\tilde{\Gamma}_B$ are the rates of escaping from the A and B metastable states, respectively, while $\overline{N}_A(t)$ and $\overline{N}_B(t)$ are the time-dependent nonequilibrium probabilities of finding the system in the same states. Thus, when defined relative to a dividing surface separating A and B, $\sigma(\mathbf{z}) = \{1,\ \mathbf{z} \in AR;\ 0,\ \mathbf{z} \in B\}$, these probabilities read

$$\overline{N}_A(t) = 1 - \overline{N}_B(t) = \int d\mathbf{z}\, \sigma(\mathbf{z}) P(\mathbf{z},t), \tag{2.2}$$

where we have assumed the system of interest to be closed, $\overline{N}_A + \overline{N}_B = 1$. Additionally, the escape rates are related to each other through the equilibrium fractions, $\tilde{\Gamma}_A N_A^e = \tilde{\Gamma}_B N_B^e$, defined by $N_M^e = \overline{N}_M(\infty)$, $M = A,\ B$. For such a closed system the phenomenological Eq. (2.1) can be reduced to one equation for the nonequilibrium fluctuation variable, $\Delta N_{ne}(t) = \overline{N}_A(t) - N_A^e$, which then yields single-exponential dynamics,

$$\frac{\Delta N_{ne}(t)}{\Delta N_{ne}(0)} = \exp(-\tilde{\Gamma} t). \tag{2.3}$$

Equation (2.3) depends upon the phenomenological kinetic rate constant, $\tilde{\Gamma} = \tilde{\Gamma}_A + \tilde{\Gamma}_B$, and, clearly, it need only be valid at long times, when the decay of a perturbation, $\Delta N_{ne}(t)$, back to equilibrium becomes unconditionally single exponential.

Since it is generally impossible to derive phenomenological rate equations like Eq. (2.1) from evolution equations like Eqs. (1.3) and (1.4), there exists no precise identification of microscopic dynamical quantities with the phenomenological rate constants. As a consequence, various methods have been devised to establish such a connection. One of the most commonly used approaches is based on the equilibrium time correlation function formalism [23,24]. Since the problem of interest can be formulated in two formally equivalent ways–namely, using the Hamiltonian representation, Eq. (2.4), and the original Fokker-Planck Eq. (1.4)–two formulations of the equilibrium correlation function formalism are possible.

A. Hamiltonian representation

To begin we consider the Hamiltonian formulation. The starting point of this approach is the observation that the Fokker-Planck dynamics, Eq. (1.4), is equivalent to the dynamics of the Hamiltonian [12]

$$H = \tfrac{1}{2} p_x^2 + U(x) + \tfrac{1}{2} \sum_i \left[p_i^2 + (\omega_i y_i - g_i x/\omega_i)^2 \right], \tag{2.4}$$

involving a bath of mass-weighted harmonic oscillators y_i bilinearly coupled to the system coordinate x. The summation in Eq. (2.4) is understood to be over an infinite set of bath oscillators tending towards a continuum. The bath parameters (frequencies ω_i and coupling constants g_i) are related to the friction coefficient γ through the expression $2\gamma\delta(t) = \Sigma_i (g_i/\omega_i)^2 \cos(\omega_i t)$. In Eq. (2.4), the system of interest is represented by a particle (a representative point) in an infinite-dimensional phase space $(\mathbf{q},\mathbf{p})$, whose axes are the positions $\mathbf{q} = (x, y_1, y_2, \ldots)$ and conjugate momenta $\mathbf{p} = (p_x, p_1, p_2, \ldots)$, the respective dynamics of which are governed by Hamilton's equations.

If the system consists of N particles, and f is a dividing surface separating reactants and products, which is defined in the full infinite-dimensional space $\mathbf{q}$, we can define the fraction of particles in state A, and state B, at time t as

$$N_A(t) = 1 - N_B(t) = \frac{1}{N} \sum_{n=1}^{N} \theta\{-f[\mathbf{q}^n(t)]\}, \tag{2.5}$$

where $\theta(x)$ is the Heaviside step function. At equilibrium, the average fraction of particles in A and in B are then $\langle N_A \rangle = N_A^e$ and $\langle N_B \rangle = N_B^e$, where the brackets denote the equilibrium ensemble average. The application of a disturbance changes the observed fractions from their equilibrium values, N_A^e and N_B^e, to time-dependent nonequilibrium values, $\langle N_A \rangle(t)$ and $\langle N_B \rangle(t)$. Recall that at the macroscopic level, the time dependence of these numbers is assumed to be characterized by the linear rate law, Eq. (2.1), and thus by single exponential decay.

It will now be our goal to link the phenomenological result (2.3) to the equilibrium time correlation function [23,24],

$$C(t) = \frac{\langle \Delta N(0) \Delta N(t) \rangle}{\langle \Delta N(0) \Delta N(0) \rangle}, \tag{2.6}$$

where $\Delta N(t) = N_A(t) - N_A^e$ is an equilibrium fluctuation of the number of particles of type A, and the brackets again denote the equilibrium ensemble average. With Eq. (2.5) this correlation function takes the form

$$C(t) = \frac{\langle \Delta\theta(0) \Delta\theta(t) \rangle}{N_A^e N_B^e}, \tag{2.7}$$

where $\Delta\theta(t) \equiv \theta\{-f[\mathbf{q}^n(t)]\} - N_A^e$, and where we have made use of the fact that for a closed system at equilibrium $\langle \Delta N(0) \Delta N(0) \rangle = N_A^e N_B^e$. Proceeding further we note that the time evolution of $C(t)$ can always be written as

$$C(t) = \sum_{m=1} c_m \exp(-\lambda_m t). \tag{2.8}$$

The summation in Eq. (2.8) is over all the characteristic frequencies, λ_m, of the full infinite-dimensional system and, by construction, the expansion coefficients c_m satisfy $\Sigma_{m=1} c_m = 1$. Due to the equivalence of the Hamiltonian [Eq. (2.4)] and the Fokker-Planck [Eq. (1.4)] representations, these frequencies λ_m are just the eigenvalues of the Fokker-Planck operator L. The coefficients, c_m, will depend upon the particular choice of the dividing surface and may in general be both positive and negative. However, in the limit of large friction where the spectrum of the Fokker-Planck operator is real, the coefficients c_m will all be positive. In this limit, one may interpret each coefficient c_m as the fraction of the excess number of particles in state A, ΔN, which decay with the

corresponding rate λ_m. Or, more explicitly, c_m represents the fraction of initial representative phase space points which relax to equilibrium (relative to the surface f) with an exponential relaxation time λ_m. If we could find the dividing surface yielding $c_1=1$, $c_{m>1}=0$, then $C(t)$ based on this dividing surface should, in fact, monitor only the slowest system mode, which is characterized by the least nonvanishing eigenvalue, λ_1. In this case alone, the relaxation dynamics of $C(t)$ will be single exponential, and thus the phenomenology will hold true at all times. Comparison of Eqs. (2.3) and (2.8) (with $c_1=1$, $c_{m>1}=0$) shows that the phenomenological rate constant $\tilde{\Gamma}$ is just λ_1, and hence we equate this least nonvanishing eigenvalue of the Fokker-Planck operator with the true kinetic rate constant Γ, i.e.,

$$\tilde{\Gamma}\equiv\Gamma=\lambda_1. \tag{2.9}$$

Unfortunately, to find such a perfect dividing surface one would have to solve the corresponding Hamilton's equations, which cannot usually be done.

In contrast to the case of the perfect dividing surface, an arbitrary dividing surface will yield multiexponential relaxation dynamics for $C(t)$ [see Eq. (2.8)]. Yet, even in this latter case $C(t)$ should decay as a single exponential at long times, since

$$C(t\gg 1/\lambda_2)=c_1\exp(-\lambda_1 t). \tag{2.10}$$

Importantly, the Onsager regression hypothesis suggests that the nonequilibrium fluctuation $\Delta N_{ne}(t)$ decays to equilibrium in the same fashion as do equilibrium fluctuations $\Delta N(t)$ of the number of particles of type A, such that

$$\frac{\Delta N_{ne}(t)}{\Delta N_{ne}(0)}=C(t). \tag{2.11}$$

At long times ($t\gg\lambda_2^{-1}$) we find, by combining Eqs. (2.10) and (2.11), that

$$\frac{\Delta N_{ne}(t)}{\Delta N_{ne}(0)}=c_1\exp(-\lambda_1 t). \tag{2.12}$$

Comparing Eq. (2.12) with Eq. (2.3) and using Eq. (2.9) shows that the phenomenology is, in general, valid at long times *if and only if* the coefficient c_1 is close to unity. If $c_1\neq 1$, then an explicit expression for this coefficient would be required to extract the rate $\Gamma=\lambda_1$ from the correlation function. This issue will be addressed in Sec. III of the present paper.

For now, we examine the implications of this result for the time-dependent *reactive flux* expression [24]

$$k_{\mathrm{RF}}(t)=-\dot{C}(t)=\frac{\langle\delta[f(0)]\dot{f}\theta[-f(t)]\rangle}{N_A^e N_B^e}, \tag{2.13}$$

which is derived from Eq. (2.7) by making use of the fact that the derivative of a step function is a Dirac delta function. The properties of the function $k_{\mathrm{RF}}(t)$ deserve to be pointed out, as Eq. (2.13) forms the basis for the standard computational method for determining reaction rate constants [26,27]. These properties are:

(i) From a computational point of view the most appealing feature of the reactive flux method is that it allows one to avoid problems arising from widely separated time scales. Such time scale separations are typical in barrier crossing processes for which the decay time $1/\Gamma=1/\lambda_1$ is usually much larger than the intrawell relaxation time (which is of the order of $1/\lambda_2$) that it takes a particle to thermalize within the part of phase space bordered by the barrier. The reactive flux method circumvents this difficulty by initiating trajectories at the barrier top, such that, by Eq. (2.13), the long time behavior may be extracted on a short time scale. Specifically, after a time t, that is longer than $1/\lambda_2$ but is much shorter than the inverse rate $1/\Gamma=1/\lambda_1$, $C(t)$ should decay by a single exponential, Eq. (2.10). Consequently, by differentiating Eq. (2.10), the reactive flux function becomes $k_{\mathrm{RF}}(t\gg 1/\lambda_2)\approx c_1\Gamma e^{-\Gamma t}$. Accordingly, for a time t_p such that $\lambda_2^{-1}\ll t_p\ll\Gamma^{-1}$, the reactive flux formula (2.13) approaches a plateau value

$$k_{\mathrm{RF}}(t_p)=\Gamma_{\mathrm{RF}}=c_1\Gamma. \tag{2.14}$$

However, it is typically assumed on basis of the phenomenology, Eq. (2.3), which when compared to Eqs. (2.10) and (2.11) gives $c_1=1$, that the reactive flux expression Γ_{RF} coincides exactly with the true rate Γ [10,21,23–27]. Yet, from Eq. (2.14), it follows immediately that this assumption will not be true unless $c_1=1$.

(ii) The zero time limit of the reactive flux expression, Eq. (2.13), is just the TST estimate of the rate for the dividing surface f (Refs. [20,21,24])

$$k_{\mathrm{RF}}(0+)=\Gamma_{\mathrm{TST}}[f]=\frac{\langle\delta(f)\dot{f}\theta(\dot{f})\rangle}{N_A^e N_B^e}. \tag{2.15}$$

Note that this limit must be taken as t goes to zero from above.

(iii) The time-dependent reactive flux, $k_{\mathrm{RF}}(t)$, is bounded from above by its zero time value, the TST rate expression for that dividing surface, Eq. (2.15), such that $k_{\mathrm{RF}}(t)\leq\Gamma_{\mathrm{TST}}[f]$. This property can be seen mathematically as follows: at any time t the function $\theta[-f(t)]$ can at most be unity. If the initial velocity $\dot{f}$ were negative, then even if $\theta[-f(t)]=1$ the net contribution will be negative, that is, it will be smaller than the contribution of 0 given for the TST estimate [$\theta(\dot{f})=0$ if $\dot{f}<0$]. On the other hand, if $\dot{f}$ is positive, when $\theta[-f(t)]$ has its maximal value of 1, $k_{\mathrm{RF}}(t)$ also has its maximal value, which is just the TST rate. Physically, this bounding property results because in TST it is assumed that all trajectories crossing the dividing surface are associated with the slowest relaxation time $1/\Gamma=1/\lambda_1$, i.e., with reaction. If an imperfect dividing surface is used, there will be surface-crossing trajectories that relax more rapidly than λ_1. These trajectories will repeatedly recross the dividing surface on the time scale of intrawell motion (λ_2 or faster) and are not associated with the reaction. Thus, Γ_{TST}, at most, *overcounts* the number of truly reactive trajectories. Consequently, since the reactive flux expression starts with the TST estimate at $t=0$, and, as time proceeds, eliminates recrossing trajectories from those counted towards the overall rate, it follows that

$$\Gamma_{RF} \leqslant \Gamma_{TST}[f]. \tag{2.16}$$

Since the only apparent approximation in the derivation of the TST method is this overcounting of recrossing trajectories, it is commonly believed that TST provides a rigorous upper bound to the rate constant. Yet, we have shown [see Eq. (2.14)] that Γ_{RF}, and thus Γ_{TST} [see Eq. (2.16)], bounds only $c_1\Gamma$ and not Γ itself. Hence, from Eq. (2.16) we see that TST also bounds $c_1\Gamma$ rather than Γ itself, as generally believed.

The above reactive flux approach is applicable only if there is a well-defined separation of time scales, since the function $k_{RF}(t)$ would otherwise go to zero without a well-defined plateau. Another disadvantage of this expression, Eq. (2.13), is that its plateau value [Eq. (2.14)] involves the coefficient c_1, which is in general not known. A way to resolve both of these problems is to employ, instead of Eq. (2.13), an alternative expression given by

$$k_C(t) = -\frac{d}{dt}\ln[C(t)] = \frac{k_{RF}(t)}{C(t)}, \tag{2.17}$$

in which the unknown factor c_1 cancels at times longer than $1/\lambda_2$. It is not difficult to see that the reactive flux so defined retains the principal advantages of the standard reactive flux method, Eq. (2.14), being free of its drawbacks. In particular, for intermediate (as well as long) times Eq. (2.17) *always* approaches a limiting value coinciding with the least nonvanishing eigenvalue [see Eq. (2.9)], i.e., with the true rate $k_C(t \gg \lambda_2^{-1}) = \lambda_1 = \Gamma$.

B. Operator representation

An alternative approach to the above problem is based on an operator representation of an equilibrium correlation function [10,26]

$$W(t) = \frac{\langle \Delta\chi(0)\Delta\varphi(t)\rangle}{N_A^e N_B^e} = \frac{\langle \Delta\chi \exp(tL^*)\Delta\varphi\rangle}{N_A^e N_B^e}, \tag{2.18}$$

whose physical significance depends on the functions χ and φ. In Eq. (2.18), $L^* = P_{eq}^{-1} L P_{eq}$ is the backward operator of the time-reversed process [3]

$$L^* = -v\frac{\partial}{\partial x} + \left[\frac{dU(x)}{dx} - \gamma v\right]\frac{\partial}{\partial v} + \frac{\gamma}{\beta}\frac{\partial^2}{\partial v^2}, \tag{2.19}$$

$\Delta\chi = \chi - \langle\chi\rangle$, and similarly for φ, while $\langle\ \rangle$ denotes the average with respect to the stationary solution $P_{eq}(x,v)$ and has the properties of an inner product, i.e.,

$$\langle \Delta\chi(0)\Delta\varphi(t)\rangle = \int d\mathbf{z}\, P_{eq}(\mathbf{z})\Delta\chi(\mathbf{z}) e^{tL^*}\Delta\varphi(\mathbf{z}). \tag{2.20}$$

Note that if the functions $\varphi(\mathbf{z})$ and $\chi(\mathbf{z})$ are both taken to be the step functions $\theta(-x)$, the correlation function $W(t)$ in Eq. (2.18) reduces to the correlation function introduced earlier, $C(t)$, Eq. (2.6), with the dividing surface taken as $f = x = 0$. More generally, although the characteristic function of the domain of attraction of the reactant state A, namely $\varphi(\mathbf{z})$, equals unity far inside the domain of attraction and zero far outside, it may show a smooth transition from these extreme values in contrast to the step function $\theta(-f)$. The function $\chi(\mathbf{z})$ is of similar nature as $\varphi(\mathbf{z})$.

The phenomenological result, Eq. (2.3), can be linked to the equilibrium time correlation function $W(t)$ in the same way as it was to $C(t)$. In particular, at long times when the phenomenology holds, $W(t)$ has the same decay as the variable $\Delta N(t)$ itself. Consequently, a corollary of the improved reactive flux expression [Eq. (2.17)] defined on the basis of $W(t)$,

$$k_W(t) = -\frac{d}{dt}\ln[W(t)], \tag{2.21}$$

should exhibit the same long time behavior as does Eq. (2.17), i.e.,

$$k_W(t \gg \lambda_2^{-1}) = \Gamma. \tag{2.22}$$

This $W(t)$-based approach has been used in both analytical [10,25] and numerical [28] calculations of rate constants. It has the advantage that $W(t)$ may be expanded in the eigenvalues of the Fokker-Planck operator with *known* coefficients, as follows below. It is this expansion which will enable us to develop an approximate expression for c_1 in Eq. (2.14), and will enable us to determine which quantity VTST does bound from above (see Sec. III B).

We begin by recognizing that the Green function of the Fokker-Planck equation can be expanded in terms of the complete set of eigenfunctions h_m, i.e.,

$$P(\mathbf{z},t|\mathbf{z}^0) \equiv e^{tL}\delta(\mathbf{z}-\mathbf{z}^0) = \sum_{m=0} P_{eq}(\mathbf{z}) h_m(\mathbf{z}) h_m^+(\mathbf{z}^0) e^{-\lambda_m t} \tag{2.23}$$

where

$$\begin{aligned} L^* h_m &= -\lambda_m h_m, \\ L^+ h_m^+ &= -\lambda_m h_m^+, \\ (h_m^+, h_n) &= \delta_{mn}. \end{aligned} \tag{2.24}$$

In the above we have introduced a scalar product of two functions having the weight function P_{eq},

$$(f,g) = \int dx\, dv\, P_{eq}(x,v) f(x,v) g(x,v). \tag{2.25}$$

Moreover, L^+ is the backward operator of the original process,

$$L^+ = v\frac{\partial}{\partial x} - \left[\frac{dU(x)}{dx} + \gamma v\right]\frac{\partial}{\partial v} + \frac{\gamma}{\beta}\frac{\partial^2}{\partial v^2}. \tag{2.26}$$

It may be noted here that this operator has the same eigenvalues λ_m as the backward operator of the time-reversed process L^* with corresponding eigenfunctions h_m^+ that are the time reversed functions of h_m, $h_m^+(x,v) = h_m(x,-v)$. Then, using that the equilibrium probability density P_{eq} satisfies

the stationary Fokker-Planck equation, $LP_{eq}=0$, such that $h_0=h_0^+=1$ and $\lambda_0=0$, one finds from substitution of Eq. (2.23) into Eq. (2.18) that

$$W(t)=\sum_{m=1} w_m \exp(-\lambda_m t), \tag{2.27}$$

where the expansion coefficients are given by

$$w_m=\frac{(\chi,h_m)(\varphi,h_m^+)}{N_A^e N_B^e}. \tag{2.28}$$

Substitution of Eq. (2.27) into Eqs. (2.21) and (2.22) yields $\Gamma=\lambda_1$ as anticipated [cf Eq. (2.9)].

The efficacy of the above approach depends crucially on a proper choice of the functions $\chi(\mathbf{z})$ and $\varphi(\mathbf{z})$. The best choice would be the eigenfunctions of L^+ and L^* corresponding to the first nonzero eigenvalue λ_1. In that case, all the coefficients w_m except w_1 would be equal to zero, and the initial value of the log-based reactive flux $k_W(0)$ would already yield the exact rate constant. An approximate eigenfunction ξ of L^* may also serve the purpose, provided that $k_W(0)$ is well defined. Indeed, setting $\varphi(\mathbf{z})=N_A^e[\xi(\mathbf{z})+1]$ and $\chi(\mathbf{z})=N_B^e[\xi^+(\mathbf{z})+1]$ ensures proper equilibrium densities N^e and leads, via Eq. (2.18), to $W(t)=\langle\xi^+\exp(tL^*)\xi\rangle$, which, via Eq. (2.21), leaves us with

$$k_W(0)=\Gamma_{\mathrm{RQ}}[\xi]=-\frac{(\xi^+,L^*\xi)}{(\xi^+,\xi)}. \tag{2.29}$$

The above equation is nothing but a Rayleigh quotient [10,11]. Bounding properties of this expression may be deduced by studying the difference $k_W(0)-k_W(\infty)$ which reads

$$k_W(0)-k_W(\infty)=\frac{\sum_{m=2} w_m(\lambda_m-\lambda_1)}{\sum_{m=1} w_m}. \tag{2.30}$$

If one assumes that λ_m are real, then the differences $\lambda_m-\lambda_1$ are positive by definition, the coefficients w_m

$$w_m=(\xi^+,h_m)(\xi,h_m^+)=(\xi^+,h_m)^2 \tag{2.31}$$

are also positive, and $k_W(0)\geqslant\lambda_1$ follows. Consequently, a *sufficient* condition for the Rayleigh quotient to provide an *upper bound* to the exact rate, i.e., for $\Gamma_{\mathrm{RQ}}[\xi]\geqslant\Gamma$, is that the spectrum of the Fokker-Planck operator be *real*, as is generally the case in the Smoluchowski limit.

C. Miscellaneous

For completeness we also mention two other possible ways to identify the phenomenological rates. One is based on the observation that $W(t)\sim\exp(-\Gamma t)$ at long times when the phenomenology is valid. A first dynamical rate expression for the phenomenological rate constant is then clearly [24]

$$\Gamma_{\mathrm{MRT}}^{-1}=\tau_{\mathrm{MRT}}=\int_0^\infty dt\, W(t)/W(0). \tag{2.32}$$

By definition, the right-hand side of the above equation is a so-called mean relaxation time, the quantity often used when studying noise-induced transitions [29,30]. With Eq. (2.27) this quantity reads

$$\Gamma_{\mathrm{MRT}}=W(0)\left(\sum_{m=1} w_m/\lambda_m\right)^{-1}. \tag{2.33}$$

On account of the separation of time scales which is inherent to barrier crossing processes and shows itself in a large gap in the spectrum of the Fokker-Planck operator separating the first nonzero eigenvalue from the rest of the spectrum, Eq. (2.33) can be written as $\Gamma_{\mathrm{MRT}}\approx\Gamma W(0)/w_1$.

A second approach is based on the mean first passage time formalism [3,4,11]. Within its scope the escape rate is determined as the inverse of the mean time τ_{MFPT} after which a stochastic trajectory starting within the well passes the stochastic separatrix for the first time, $\Gamma_{\mathrm{MFPT}}=\tau_{\mathrm{MFPT}}^{-1}$. This reduces Eqs. (1.3) and (1.4) to the stationary backward Fokker-Planck equation supplemented by absorbing boundary conditions. However, since the spectrum of the Dirichlet problem is in general different from that of the Neumann problem, it is difficult to connect Γ_{MFPT} with the other rate expressions, Eqs. (2.9), (2.22), and (2.32).

III. VTST AND RAYLEIGH QUOTIENT METHODS

In this section, explicit expressions for the rate are derived for both the VTST and the Rayleigh quotient method, in order to elucidate the relationship between these two methods. For simplicity we restrict our considerations to a symmetric double well, $U(x)=U(-x)$. In such a case, the forward and backward rates are equal and $\Gamma=2\Gamma_A$. The generalization to an arbitrary bistable potential is straightforward. One may also note that our presentation can be extended to systems with memory friction.

A. Transition state theory

As noted, the starting point of the VTST method is the TST rate, Eq. (2.15). An explicit expression for this rate reads

$$\Gamma_{\mathrm{TST}}[f]=\frac{4\int d\mathbf{q}d\mathbf{p}\,\delta(f)(\mathbf{v}\cdot\nabla f)\theta(\mathbf{v}\cdot\nabla f)e^{-\beta H}}{\int d\mathbf{q}d\mathbf{p}\,e^{-\beta H}}, \tag{3.1}$$

where the Dirac delta function $\delta(f)$ limits the integration to the dividing surface $f=0$, the gradient of the surface, ∇f, is in the full infinite-dimensional phase space $(\mathbf{q},\mathbf{p})$, and $\mathbf{v}$ is the generalized velocity vector in phase space with components $(\dot{x},\dot{p}_x,\dot{y}_1,\dot{p}_1,\ldots)$. When writing Eq. (3.1) we used the fact that for a symmetric double well the equilibrium populations of reactants and products are $N_A^e=N_B^e=\frac{1}{2}$, independent of the dividing surface [18]. The standard one-dimensional TST rate

$$\Gamma_{\mathrm{TST}}=\left\{\sqrt{\tfrac{1}{2}\pi\beta}\int_{-\infty}^0 dx\, e^{\beta[U(0)-U(x)]}\right\}^{-1} \tag{3.2}$$

is obtained from Eq. (3.1) by taking the dividing surface to be of the form $f=x=0$. A commonly used approach, VTST, is to perform the integration of Eq. (3.1) over various trial surfaces and to select the smallest crossing rate as the best approximation to the true rate [13]. The latter may be achieved either by trial and error or by selecting a trial surface f depending on a set of free parameters, which may be varied to yield a minimum rate. Following Talkner and Pollak [22] we choose the dividing surface to be planar such that

$$f=a_0x+\sum_{i=1} a_iy_i, \tag{3.3}$$

where the coefficients a_i are the components of the unit vector ∇f perpendicular to the dividing surface and are therefore normalized

$$\sum_{i=0} a_i^2=1. \tag{3.4}$$

Substituting Eq. (3.3) into (3.1) and varying the resulting rate expression $\Gamma_{\mathrm{VTST}}[a_0,a_1,\ldots]$ with respect to the coefficients a_i, one obtains (for more details see Ref. [19])

$$a_i=a_0g_i/(\omega_i^2+\mu^2),$$
$$a_0=\sqrt{2\mu/(2\mu+\gamma)}. \tag{3.5}$$

Thus, the problem of finding the optimal planar dividing surface [the set of transformation coefficients $(a_0,a_1,\ldots)$] reduces to finding a *single* effective frequency μ. The latter in turn is to be fixed by minimizing $\Gamma_{\mathrm{VTST}}[\mu]$, a procedure that results in a self-consistent integral equation of the form

$$\int_{-\infty}^{\infty} dx[\gamma-\beta\mu(\mu+\gamma)(2\mu+\gamma)x^2] \times\exp[-\beta U(x)-\beta\mu(\mu+\gamma)^2x^2/\gamma]=0. \tag{3.6}$$

This equation must be solved numerically to find the effective frequency μ.

To simplify comparison with the Rayleigh quotient method we define a variable ω such that

$$\mu=\sqrt{\omega^2+\gamma^2/4}-\gamma/2, \tag{3.7}$$

which leads us to

$$\Gamma_{\mathrm{VTST}}[\omega]=\frac{2}{\pi Z}\sqrt{\frac{\mu(\omega^2+\mu^2)}{\gamma}}\int_{-\infty}^{\infty}dx \times\exp\left[-\beta U(x)-\frac{\beta\omega^4}{\mu\gamma}x^2\right]. \tag{3.8}$$

The variational parameter is now the effective barrier frequency ω, rather than μ, and is determined by Eq. (3.6) through Eq. (3.7). Notice that Eq. (3.8) is simply a VTST rate expression in which the system parabolic barrier frequency ω, which changes as the dividing surface is rotated, is used as the variational parameter [22]. Indeed, for each planar dividing surface there exists a corresponding parabolic barrier frequency, which determines the slope α of the effective deterministic separatrix in phase space, $x=\alpha(\omega)v$ (see Fig. 2). Minimizing $\Gamma_{\mathrm{VTST}}[\omega]$ with respect to ω is thus identical to optimizing the rate constant $\Gamma_{\mathrm{VTST}}[a_0,a_1,\ldots]$ with respect to the coefficients a_i, or, in other words, to optimizing the slope of the separatrix α.

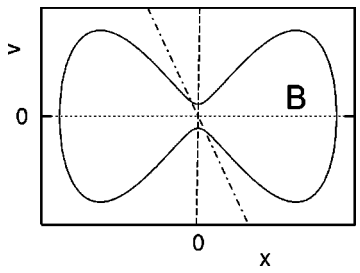

FIG. 2. Schematic representation of the VTST optimization procedure. Solid line, equipotential $v^2/2+U(x)=\mathrm{const}$; dashed line, TST dividing surface $x=0$; dot-dashed line, optimized dividing surface $x=\alpha v$.

Before closing three remarks are in order. First, in the weak friction limit ($\gamma\to 0$) where the true rate falls off with decreasing γ, $\Gamma_{\mathrm{VTST}}[\omega]$ becomes insensitive to the variational parameter, approaching the standard TST rate, Eq. (3.2), independent of (any finite) ω. Consequently, Eq. (3.8) is applicable only in the spatial diffusion regime, i.e., as long as the true rate keeps increasing with decreasing friction coefficient. Second, we note that for $\gamma>0$, Eq. (3.6) may give more than one solution. Therefore, one must determine which solution leads to the minimum of the rate constant and identify this solution with Γ_{VTST}. Third, for a double well potential with a *parabolic* barrier $[U(x)=U(0)-(1/2)\omega_b^2x^2+O(x^3)]$ the calculation may be substantially simplified by setting ω equal to the barrier frequency [17], $\omega=\omega_b$, in which case the effective frequency μ becomes identical to the standard Kramers-Grote–Hynes reactive frequency, as given by Eq. (3.7) with $\omega=\omega_b$. Such a simple choice of the dividing surface, although in general not fully optimized, is unconditionally justified in the high-barrier (low-temperature) limit where one may safely ignore the anharmonicity of the potential.

B. Relation of the Rayleigh quotient method to VTST

The Rayleigh quotient, Eq. (2.29), also provides a variational methodology for determining the rate, $\Gamma=\lambda_1$, if the function ξ is taken as a variational trial function, i.e., $\Gamma[\xi]=\Gamma_{\mathrm{RQ}}[\xi]$. In Sec. II we saw that when $\xi=h_1$, the true eigenfunction, Eq. (2.29) yields the true eigenvalue, and thus the more accurate is the trial function the more accurate will be the estimate for the rate. Although there exist a number of different Rayleigh quotient expressions [9–11,22], the above approach, formulated by Talkner [10,11], has the advantage that it is variational in the whole friction range. By this we mean that a first-order error in the trial function leads to a second-order error for the rate. However, as noted earlier, Eq. (2.29) only gives a rigorous upper bound to the rate when the spectrum of eigenvalues is real. The latter is in general true for strong friction ($\gamma\gg\omega_b$) and may not be the case in the intermediate-to-weak friction regime ($\gamma\lesssim\omega_b$).

To elucidate the relationship between the VTST and Rayleigh quotient estimates for the rate we follow Talkner and Pollak [22] and restrict ourselves to the Kramers trial function [6]. The derivation of this function is based on the idea that at vanishing temperature ($\beta\to\infty$) the solutions of the resulting first-order partial differential equation are piecewise constant on the domains of reactants and products. We choose these values to be $+1$ and -1, such that the resulting function is normalized and orthogonal to the stationary solution. For low temperatures the presence of the small diffusive term in L^* changes the behavior of the eigenfunction h_1 only near the deterministic separatrix where the steplike behavior is smoothed out and it is therefore only in this region that h_1 differs from the stationary solution, $h_0=1$. Thus, for sufficiently small β^{-1} only the barrier region contributes to the Rayleigh quotient (2.29), because this expression contains the stationary distribution as a weight. Hence, it is useful to rewrite the true potential as a sum of a parabolic barrier potential $U_{\rm pb}(x)=-\frac{1}{2}\omega^2x^2$, with the frequency ω being a free (variational) parameter, and a reminder $U(x)+\frac{1}{2}\omega^2x^2$. It is then not difficult to show [6] that the corresponding operator $L^*_{\rm pb}$ has a nontrivial eigenfunction ξ associated with a zero eigenvalue whose form is

$$\xi(x,v)=\sqrt{\frac{2\beta}{\pi\mu\gamma}}\int_0^{\mu v-\omega^2 x}ds\,\exp\left(-\frac{\beta s^2}{2\mu\gamma}\right), \tag{3.9}$$

which is just the so-called Kramers trial function. Substitution of Eq. (3.9) into the numerator of the Rayleigh quotient (2.29) yields

$$\begin{aligned}(\xi^+,L^*\xi)=\frac{1}{\gamma Z}\sqrt{\frac{2\beta^3}{\pi^3}}\int_{-\infty}^{\infty}dx\ \int_{-\infty}^{\infty}dy\ \left[\frac{dU(x)}{dx}+\omega^2x\right]\\ \times\exp\left\{-\tfrac{1}{2}\beta\left[2U(x)+\omega^2x^2+\frac{\omega^2y^2}{\omega^2-\mu^2}\right]\right\}\\ \times\int_0^{\mu y+(\omega^2+\mu^2)x}ds\,\exp\left(-\frac{\beta s^2}{2\mu\gamma}\right),\end{aligned} \tag{3.10}$$

where we have performed the derivative with respect to v and replaced v by the variable $y=v-\mu x$. A partial integration over x allows one to get rid of the s integral. The resulting integral over y is Gaussian and therefore can be performed analytically leading us to

$$(\xi^+,L^*\xi)=\Gamma_{\rm VTST}[\omega], \tag{3.11}$$

where $\Gamma_{\rm VTST}[\omega]$ is given by Eq. (3.8). This immediately gives

$$\Gamma_{\rm RQ}[\omega]=\frac{\Gamma_{\rm VTST}[\omega]}{(\xi^+,\xi)}. \tag{3.12}$$

It is thus seen that the Rayleigh quotient rate expression based on the Kramers trial function, $\Gamma_{\rm RQ}[\omega]$ differs from the VTST rate based on a planar dividing surface, $\Gamma_{\rm VTST}[\omega]$, by the denominator in Eq. (3.12) that satisfies the inequality

$$(\xi^+,\xi)\leqslant 1. \tag{3.13}$$

For a symmetric double well, Eq. (4.1), over a wide range of the variational parameter ($\omega\gtrsim\omega_b$) this denominator can be well approximated by

$$(\xi^+,\xi)\approx 1-e^{-\beta E}, \tag{3.14}$$

where E is the barrier height. Consequently, the identity shown by Talkner and Pollak [22] can be recovered only in the low-temperature limit ($\beta\to\infty$) where the denominator (ξ^+,ξ) becomes equal to unity. This latter result can be obtained from Eq. (2.25) by realizing that the trial function $\xi(x,v)$, Eq. (3.9), reduces to a piecewise function $2\theta(\mu v-\omega^2x)-1$ as $\beta\to\infty$. Outside of the low-temperature limit, Eq. (3.12) leads us to conclude, in contrast with the conclusion of Talkner and Pollak, that VTST *does not* possess the bound property inherent to the Rayleigh quotient method in the Smoluchowski limit $\gamma\to\infty$. The latter is consistent with our earlier finding, Eqs. (2.14) and (2.16), that VTST bounds $\Gamma_{\rm RF}=c_1\Gamma$ rather than the rate Γ itself. Although this failure of the VTST bounding properties is revealed using the restricted set of dividing surfaces $\{f\}$, Eq. (3.3), we are assured that $\Gamma_{\rm VTST}$ optimized from an unrestricted set $\{\tilde f\}$, which may include different types of both planar and curved dividing surfaces [18] will also fail to bound the true rate, since by definition the unrestricted result $\Gamma_{\rm VTST}[\tilde f]$ is smaller than $\Gamma_{\rm VTST}[f]$.

Thus, to see which quantity the VTST rate does bound from above, one has to determine the coefficient c_1. This can be achieved by establishing a connection between the zero time limits of the derivatives $\dot C(t)$ and $\dot W(t)$ underlying VTST and the Rayleigh quotient method, respectively. If VTST is restricted to planar dividing surfaces, Eq. (3.3), while the Rayleigh quotient method is limited to the class of Kramers trial functions, Eq. (3.9), one immediately obtains via Eqs. (2.15), (2.29), and (3.11) that $\dot W(0+)$ equals $\dot C(0+)$, $\dot W(0+)=\dot C(0+)=\Gamma_{\rm VTST}[\omega]$. That is, the two correlation functions become similar in this case, allowing us to estimate the unknown coefficient c_1 as $c_1=w_1$, such that from Eq. (2.31),

$$c_1=(\xi^+,h_1)^2. \tag{3.15}$$

The above equation involves the true eigenfunction h_1 whose closed form expression is not known exactly. However, our calculations show [see, e.g., Fig. 6 in Sec. IV] that in the spatial diffusion regime this eigenfunction can be well approximated by the normalized Kramers trial function

$$h_1(x,v)\approx\frac{\xi(x,v)}{\sqrt{(\xi^+,\xi)}}, \tag{3.16}$$

which gives

$$c_1\approx(\xi^+,\xi)\equiv c_{1\xi}. \tag{3.17}$$

The approximate coefficient $c_{1\xi}$ is nothing but the denominator of the Rayleigh quotient rate expression, Eq. (3.12), which is typically $c_{1\xi}>0$ for $\gamma>\omega_b$. It then follows that $\Gamma_{\rm VTST}=c_{1\xi}\Gamma_{\rm RQ}$, and, since $\Gamma_{\rm VTST}\geqslant c_1\Gamma$ [by Eqs. (2.14) and (2.16)], that

$$\Gamma_{\mathrm{RQ}} \geqslant (c_1/c_{1\xi})\Gamma. \tag{3.18}$$

It is thus seen that, for *any* value of the friction coefficient, the Rayleigh quotient will necessarily bound the true rate from above *only* if the approximate estimate of c_1, $c_{1\xi}$, is less than or equal to the true value, $c_{1\xi} \leqslant c_1$. The bounding property of Γ_{VTST}, however, is more difficult to satisfy, since in this case it is c_1 rather than $c_1/c_{1\xi}$, which must be greater than or equal to 1. Since c_1 is generally not known [see Eq. (3.15)], these are not particularly useful bounding properties. However, in the zero-temperature (high-barrier) limit, Eq. (3.16) with ξ taken at $\omega=\omega_b$ becomes exact and $c_1 \to c_{1\xi}$, such that $\Gamma_{\mathrm{RQ}} \geqslant \Gamma$. Similarly, one can show that $c_{1\xi} \to 1$, and therefore that $c_1 \to 1$ in this same limit, such that $\Gamma_{\mathrm{VTST}} \geqslant \Gamma$. On the other hand, we see that, while both Γ_{RQ} and Γ_{VTST} will bound the true rate in the high-barrier limit, Γ_{VTST} is expected to loose its bounding property more rapidly than does Γ_{RQ} as the barrier height (inverse temperature) decreases because $\Gamma_{\mathrm{RQ}}=\Gamma_{\mathrm{VTST}}/c_{1\xi} \geqslant \Gamma_{\mathrm{VTST}}$.

IV. COMPARISON OF VTST AND THE RAYLEIGH QUOTIENT METHOD WITH NUMERICAL RESULTS

The validity of the above analysis is tested by comparing Eqs. (3.8) and (3.12) with exact (analytical and numerical) results for the rate. As both formulas are applicable only in the spatial diffusion regime, we restrict our consideration to $\gamma > \omega_b$. The potential is taken to be a symmetric quartic double well

$$U(x)=E(x^2-1)^2, \tag{4.1}$$

with a barrier of height E and frequency $\omega_b = 2\sqrt{E}$.

A. Smoluchowski limit

Exact results for the rate may be easily obtained only for a one-dimensional Fokker-Planck process. Therefore, it is instructive to begin our comparison in the strong friction limit where the Fokker-Planck Eq. (1.4) reduces to the one-dimensional Smoluchowski Eq. (1.7). It may be noted that for a Smoluchowski operator, the time-reversal operation reduces to the identical transformation; accordingly, $L^+ = L^*$ and $h^+(x)=h(x)$. The numerical basis set scheme we have employed to generate highly accurate results for the least nonvanishing eigenvalue $\Gamma=\lambda_1$ and the associated eigenfunction h_1 is described elsewhere [31]. This calculation provides the benchmark against which we test the Rayleigh quotient and VTST rate theories. Also, since the Smoluchowski operator L^* is Hermitian, its spectrum is real, and therefore the Rayleigh quotient provides a rigorous upper bound to the first nonzero eigenvalue in this limit (regardless of c_1). This bound holds true for any normalizable trial function that is orthogonal to the stationary distribution $P_{eq}(x) = Z^{-1}\exp[-\beta U(x)]$.

For completeness, we also include comparison with the two other dynamical approaches to the rate constant discussed in Sec. II C. In the Smoluchowski limit, the kinetic rate in a symmetric double-well potential may be given by the inverse of the mean first passage time, after which a stochastic trajectory starting at one of the local minimum values, say, at $x=1$, reaches the top of the barrier at $x=0$

$$\Gamma_{\mathrm{MFPT}}^{-1} = \gamma\beta \int_0^1 dx \int_x^\infty dy\, e^{\beta[U(x)-U(y)]}. \tag{4.2}$$

Analogously, the mean relaxation time formalism, Eq. (2.32), yields an explicit rate formula which reads [29,30]

$$\Gamma_{\mathrm{MRT}}^{-1} = 2\gamma\beta Z^{-1} \int_0^\infty dx\, e^{\beta U(x)} \left[\int_x^\infty dy\, e^{-\beta U(y)} \right]^2. \tag{4.3}$$

It may be noted that in deriving Eq. (4.3) we have set for simplicity $\xi(x)=\varphi(x)=\theta(-x)$. Moreover, since the coefficients w_m entering Eq. (2.33) are all positive in the Smoluchowski limit, the rate expression Γ_{MRT} gives an upper bound to the least nonvanishing eigenvalue in this case, $\lambda_1 \leqslant \Gamma_{\mathrm{MRT}}$.

In the strong friction limit, $\gamma \to \infty$, $\mu=\omega^2/\gamma$, and the Rayleigh quotient and VTST rate expressions, Eqs. (3.8) and (3.12), take the form

$$\Gamma_{\mathrm{RQ}}[\omega] = \frac{\displaystyle\int_{-\infty}^{\infty} dx\, e^{-\beta U(x)-\beta\omega^2 x^2}}{\displaystyle\beta\gamma \int_{-\infty}^{\infty} dx\, e^{-\beta U(x)} \left(\int_0^x dy\, e^{-\beta\omega^2 y^2/2} \right)^2}, \tag{4.4}$$

and

$$\Gamma_{\mathrm{VTST}}[\omega] = \frac{2\omega^2}{\pi\gamma Z} \int_{-\infty}^{\infty} dx\, e^{-\beta U(x)-\beta\omega^2 x^2}, \tag{4.5}$$

respectively. Before comparing these rates with $\Gamma=\lambda_1$, let us analyze how the VTST rate expression depends on the variational parameter ω. First, one sees that $\Gamma_{\mathrm{VTST}}[\omega \to 0] = 2\omega^2/\pi\gamma \to 0$, such that the VTST rate expression has a global minimum at $\omega=0$, $\Gamma_{\mathrm{VTST}}[\omega=0]=0$. This solution, which results from the failure of the method of Lagrangian multipliers used to derive Eq. (3.5) at $\omega=0$, is invalid, as it does not satisfy the normalization condition [see Eqs. (3.4) and (3.5)]. Second, as evidenced by Fig. 3(a), when the variational parameter increases, $\Gamma_{\mathrm{VTST}}[\omega]$ increases to a local maximum followed by a local minimum if the barrier is high, whereas it increases only monotonically for low barriers. Thus, we have to opt for the solution of Eq. (3.6) that leads to the smallest *nonzero* rate constant, if such a solution exists, as it does for high barriers. We refer to this solution as the true VTST rate, and to the VTST estimate for the rate obtained with $\omega=\omega_b$ as the simple VTST rate expression. Note that only this latter result can be computed in the low barrier limit.

On the other hand, Fig. 3(b) demonstrates that no such false minima are found in the Rayleigh quotient method. The corresponding rate expression, Eq. (4.4), has a nontrivial global minimum at all barrier heights. The functional $\Gamma_{\mathrm{RQ}}[\omega]$ varies from $\Gamma_{\mathrm{RQ}} = (\beta\gamma\langle x^2\rangle)^{-1}$ at $\omega=0$, reaches a minimal value near $\omega=\omega_b$, and then linearly increases as $\omega \to \infty$.

Figure 4(a) confirms that the simple VTST rate $\Gamma_{\mathrm{VTST}}[\omega_b]$ does not possess an upper bound property, in contrast to the Rayleigh quotient method, which does [Fig. 4(b)]. Indeed, simple VTST considerably underestimates the true rate, λ_1, in the limit of moderate to low barriers, βE

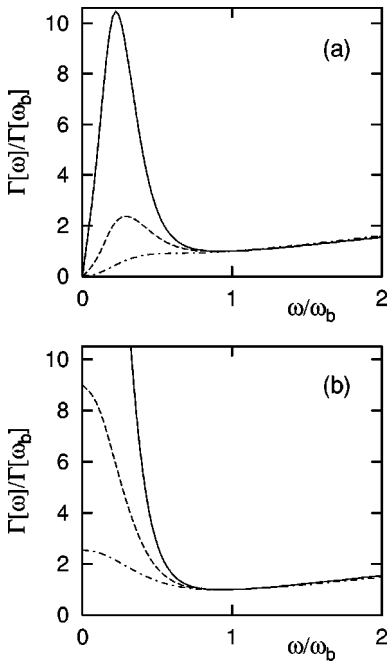

FIG. 3. Ratio $\Gamma[\omega]/\Gamma[\omega_b]$ as a function of the variational parameter ω. The calculation is performed in the strong friction Smoluchowski limit for a double well potential, Eq. (4.1) with $\beta E=2$ (dot-dashed lines), 4 (dashed lines), and 6 (solid lines). (a) VTST rate, Eq. (4.5); (b) Rayleigh quotient, Eq. (4.4).

$\leqslant 4$, and slightly overestimates it for $\beta E>4$. It is also seen that the VTST method does not bound either of the two other dynamical expressions for the rate discussed above, Γ_{MFPT} [Eq. (4.2)] and Γ_{MRT} [Eq. (4.3)]. The situation becomes worse if one uses the true VTST rate. By definition, this rate

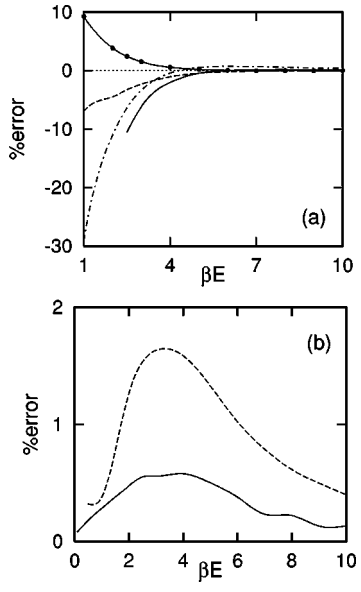

FIG. 4. Percentage errors, $100\times$(approximate−exact)/exact, in the least nonvanishing eigenvalue of the Smoluchowski operator, Eqs. (1.7) and (4.1), made by using different rate expressions. (a) Dot-dashed line, simple VTST rate expression $\Gamma_{\mathrm{VTST}}[\omega_b]$; solid line, true VTST rate; dashed line, Γ_{MFPT}, Eq. (4.2); solid line with circles, Γ_{MRT}, Eq. (4.3). (b) Solid line, results obtained by minimizing $\Gamma_{\mathrm{RQ}}[\omega]$; dashed line, $\Gamma_{\mathrm{RQ}}[\omega_b]$.

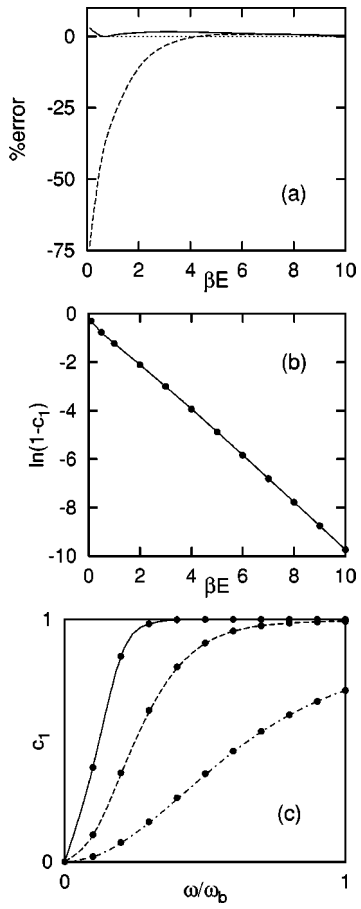

FIG. 5. (a) Percentage errors made by $\Gamma_{\mathrm{VTST}}[\omega_b]$ in comparison to the least nonvanishing eigenvalue λ_1 (dashed line) and in comparison to the standard reactive flux formula computed from $\Gamma_{\mathrm{RF}}=c_1\lambda_1$ with c_1 given by Eq. (3.15) (solid line). (b) Logarithm of the deviation of the reactive flux coefficient c_1 from unity when $\omega=\omega_b$. The solid line and circles are for results obtained in terms of Eq. (3.15) and (3.17), respectively. (c) Coefficient c_1, Eq. (3.15), as a function of the variational parameter ω for $\beta E=1$ (dot-dashed line), 5 (dashed line), and 20 (solid line). Circles are for analogous results obtained with $c_{1\xi}$, Eq. (3.17).

is smaller than $\Gamma_{\mathrm{VTST}}[\omega_b]$, and we see it already underestimates λ_1 at $\beta E=5$. Additionally, for $\beta E<2.5$ the functional $\Gamma_{\mathrm{VTST}}[\omega]$ has no nontrivial minimum and thus its minimization [with such a planar dividing surface, Eq. (3.3)] fails to provide any result for the rate at all.

On the other hand, we know that by construction VTST gives an upper bound to the standard reactive flux expression Γ_{RF} [see Eqs. (2.14) and (2.16)], which differs from the true rate Γ by the factor c_1 defined by Eq. (3.15). In Fig. 5(a) we compare VTST with both rates $\Gamma_{\mathrm{RF}}=c_1\lambda_1$ and $\Gamma=\lambda_1$. For simplicity the calculation is performed for $\omega=\omega_b$. As anticipated, $\Gamma_{\mathrm{VTST}}[\omega_b]$ systematically overestimates the standard reactive flux formula Γ_{RF} at all barrier heights even in the extreme limit of vanishing barrier $\beta E\to 0$, where VTST underestimates the exact rate by more than 75%. Additionally, the true VTST rate (not shown) exhibits the same bounding properties as does $\Gamma_{\mathrm{VTST}}[\omega_b]$. We have thus confirmed that the failure of VTST for low barriers is also inherent to the standard reactive flux method, and that this failure can be traced to the coefficient c_1, Eq. (3.15), and its

dependence on the reduced barrier height βE, see Fig. 5(b). The logarithmic plot clearly demonstrates that with increasing βE the coefficient c_1 approaches unity exponentially [cf Eq. (3.14)] so that for $\beta E \gtrsim 10$ the standard reactive flux formula Γ_{RF} becomes practically indistinguishable from the true rate Γ. For completeness we also show in Fig. 5(c) c_1 as a function of the variational parameter. As anticipated, this quantity noticeably deviates from unity for both low barriers ($\beta E \lesssim 3$) and low values of the variational parameter ($\omega \ll \omega_b$). In either of these two limits both the standard reactive flux method and VTST will fail. Away from the limit $\omega \to 0$, for a very high barrier ($\beta E = 20$), c_1, and thus the reactive flux result, remain independent of the variational parameter ω (invariant with respect to the precise definition of the dividing surface f). For a moderate barrier ($\beta E = 5$) the reactive flux is insensitive to the variational parameter only for $\omega \gtrsim \omega_b$, while for a low barrier ($\beta E = 1$) the method looses its invariance with respect to the definition of the dividing surface. It is also worth noticing the excellent agreement attained between the coefficient c_1 calculated in terms of the numerically exact eigenfunction h_1, Eq. (3.15), and its Kramers trial function approximation $c_{1\xi}$, Eq. (3.17), in this Smoluchowski limit. The agreement is seen to hold for all barrier heights and all values of the variational parameter ω.

The results presented in Figs. 3–5 confirm our analytic findings, i.e., that although VTST *does* bound the reactive flux result, Eq. (2.16), neither the reactive flux method nor VTST provide a rigorous upper bound to the least nonvanishing eigenvalue. Consequently, VTST cannot be unequivocally assumed to provide a rigorous upper bound to all systems. Perhaps more interestingly, Fig. 5 shows that c_1 decreases with the variational parameter ω as well as with the barrier height, which means that as the planar dividing surface is rotated in the full phase space (to smaller ω), the fraction of initial phase space points (in the dividing surface) which relax according to λ_1 must be decreasing. Indeed, this decrease in c_1 proceeds smoothly to the nonphysical (ill-defined) limit at $\omega = 0$ (for all barrier heights), where the normalization condition [Eq. (3.4)] fails. Thus, in some sense, the planar dividing surface is failing–for both VTST and the reactive flux method – as $\omega \to 0$, an issue we will address in more depth in a future work. For now, we recognize simply that the dependence of c_1 on ω and on the system properties (such as the barrier height) enter Eq. (3.15) through the trial function ξ and the stationary distribution function P_{eq}, respectively. Additionally, the failure of the VTST and reactive flux bounds in the $\omega \to 0$ limit corresponds to a coincident failure of the Kramers trial function ξ, Eq. (3.9), which reduces to zero and therefore becomes unnormalized in this limit.

Most importantly, however, is the result (Fig. 5) that if the barrier height is not sufficiently high, the coefficient c_1 may noticeably deviate from unity even for $\omega = \omega_b$, i.e., in the vicinity of the relevant minimum of the VTST rate expression. The latter failure arises because the equilibrium distribution is such that the rate is no longer independent of the precise definition of the metastable states, although the escape dynamics may still be governed by a single least nonvanishing eigenvalue that is well separated from the rest of the finite eigenvalues. This indicates that the phenomenological rate description as a whole looses its meaning away from the limit of high barriers, $\beta E \to \infty$. As evidenced by Fig. 4, the existing dynamical expressions for the rate (λ_1, Γ_{MFPT}, and Γ_{MRT}) coincide with each other only for $\beta E > 8$ for the symmetric quartic potential considered. For lower barriers these rates differ, even though there is still a well defined separation of time scales of the order of $\lambda_2/\lambda_1 \approx 10^3$, e.g., for $\beta E = 7$.

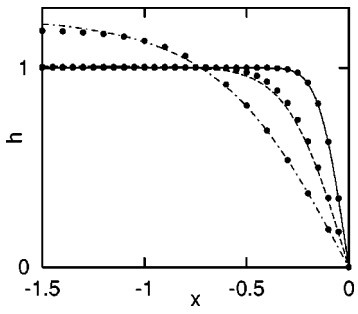

FIG. 6. Eigenfunction $h(x)$ corresponding to the first nonzero eigenvalue of the Smoluchowski operator, Eqs. (1.7) and (4.1) with $\beta E = 1$ (dot-dashed line), 5 (dashed line), and 20 (solid line). Circles are for the normalized Kramers trial function $\xi_{\mathcal{N}}(x)$, Eq. (4.6) with $\omega = \omega_b$.

In contrast to the VTST and standard reactive flux methods, the Rayleigh quotient method incorporates the factor $c_{1\xi} = (\xi^+, \xi) \approx c_1$ directly, and hence it systematically overestimates the least nonvanishing eigenvalue regardless of the reduced barrier height, as shown in Fig. 4(b). We can gain more insight into the meaning of c_1 and thus into the escape dynamics by comparing the normalized Kramers trial function $\xi_{\mathcal{N}}$, reading

$$\xi_{\mathcal{N}}(x) = \frac{\int_x^0 dy\, e^{-\beta\omega^2 y^2/2}}{\left[\int_{-\infty}^{\infty} dx\, e^{-\beta U(x)} \left(\int_0^x dy\, e^{-\beta\omega^2 y^2/2}\right)^2\right]^{1/2}}, \tag{4.6}$$

with the numerically exact results for this eigenfunction, as shown in Fig. 6. (Note that for simplicity the free parameter ω was taken to be $\omega = \omega_b$.) Since the eigenfunction $h_1(x)$ is antisymmetric, $h_1(-x) = -h_1(x)$, only results for $x \leq 0$ are presented in the figure. First, it is seen that the normalized Kramers function $\xi_{\mathcal{N}}$ [Eq. (4.6)] is in excellent agreement with the exact eigenfunction $h_1(x)$ for all temperatures, from the low $\beta E = 20$ through the very high temperature $\beta E = 1$. Second, it is clear that in the limit of extremely low temperature (high barrier), $\beta E \to \infty$, both functions $\xi_{\mathcal{N}} = h_1(x)$ slowly approach the steplike function $2\theta(-x) - 1$ underlying the standard TST rate, Eq. (3.2).

Finally, we would like to note the accuracy of the Rayleigh quotient method in this large γ-limit. As evidenced by Fig. 4(b), the relative error made in λ_1 by using $\Gamma_{\mathrm{RQ}}[\omega]$ remains lower than 0.5% for all values of βE including the limit of vanishing barrier, $\beta E \to 0$. It is also remarkable that the analytical rate formula $\Gamma_{\mathrm{RQ}}[\omega_b]$ is only slightly worse than estimates for the rate obtained by minimizing $\Gamma_{\mathrm{RQ}}[\omega]$, showing a maximal difference of 1.7%.

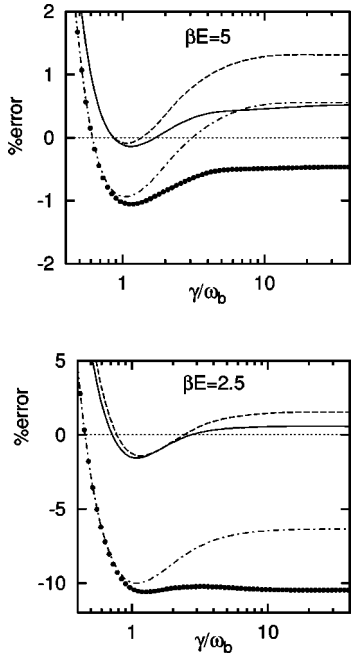

FIG. 7. Percentage errors in the least nonvanishing eigenvalue of the Fokker-Planck operator, Eqs. (1.4) and (4.1) with $\beta E=2.5$ and 5, made by using VTST and the Rayleigh quotient method. Circles and solid lines are for results obtained by minimizing $\Gamma_{\mathrm{VTST}}[\omega]$, Eq. (3.8), and $\Gamma_{\mathrm{RQ}}[\omega]$, Eq. (3.12), respectively. Dot-dashed and dashed lines are, respectively, for the simple rate formulas $\Gamma_{\mathrm{VTST}}[\omega_b]$ and $\Gamma_{\mathrm{RQ}}[\omega_b]$.

B. Full friction range

For moderate friction, $\gamma>\omega_b$, as long as the escape dynamics are dominated by spatial diffusion across the barrier top, the observed dependence of the predicted rates on the variational parameter remains the same as in the limit of strong friction $\gamma\to\infty$. The only difference at moderate friction is in the limiting values. While the VTST rate functional still has a global minimum at $\omega=0$ of $2\omega^2/(\pi\gamma)=0$, it approaches the TST rate (3.2) as $\omega\to\infty$. Similarly, the Rayleigh quotient now varies from $\Gamma_{\mathrm{RQ}}[0]=(\beta\gamma\langle x^2\rangle-1/\gamma)^{-1}$, through a minimum, to the TST rate as $\omega\to\infty$.

Estimations of the rate obtained in terms of VTST and the Rayleigh quotient method have been compared with numerically exact results for the least nonvanishing eigenvalue reported in Refs. [28] and [32]. The calculations were performed for the potential (4.1) with $\beta E=1.25$, 2.5, 5, and 10 using a path integral method described elsewhere [28,33]. We have found that for a high barrier ($\beta E=10$) both methods overestimate the least nonvanishing eigenvalue in the whole friction range. As anticipated, excellent agreement is attained in the spatial diffusion regime, $\gamma\gtrsim\omega_b$, in which case theoretical predictions deviate from exact numerical results by only $\sim 0.1\%$. Larger deviations are observed in the weak friction regime, $\gamma\lesssim\omega_b$. These deviations arise because the slow energy diffusion process, which causes the rate to fall off with decreasing γ is not accounted for by the VTST and Rayleigh quotient methods.

Away from the high-barrier limit, both methods are found to yield rates that drop below λ_1 (see Fig. 7), that is, the bounding properties of both methods fail for moderate γ. However, the VTST result drops below the exact rate more rapidly than does the Rayleigh quotient result, as anticipated since the latter is related to the former according to $\Gamma_{\mathrm{RQ}}=\Gamma_{\mathrm{VTST}}/c_{1\xi}$, Eq. (3.12), where the coefficient $c_{1\xi}$, which is at most unity [Eq. (3.13)], decreases with decreasing barrier height as $1-\exp(-\beta E)$, Eq. (3.14). Thus, although the Rayleigh quotient method does indeed bound the VTST result (within the aforementioned restrictions), it does *not* preserve its upper bound property in the range of moderate friction where the Fokker-Planck operator (1.4) is in general non-Hermitian [34]. Despite this qualitative similarity, quantitative differences between the two methods appear as the barrier is lowered. The relative error of the true VTST rate expression increases with decreasing βE much more rapidly than does the error of the Rayleigh quotient result; for $\beta E=2.5$ VTST underestimates the exact numerical rate by more than 10% as compared to 1.5% for the Rayleigh quotient method. With further decreases in the barrier height the true VTST method fails completely, as expected since the VTST rate functional $\Gamma_{\mathrm{VTST}}[\omega]$ ceases to have a nontrivial minimum in this limit. In contrast, the Rayleigh quotient result is, at worst, 6.6% below the true rate even for the extremely low barrier of $\beta E=1.25$ (not shown). Additionally, the Rayleigh quotient method restores its bounding property as γ becomes large, whereas VTST does not provide a rigorous upper bound to the rate in this limit. Finally, we note that the analytical rate formula $\Gamma_{\mathrm{RQ}}[\omega_b]$ is again only slightly worse than the full variational result.

V. CONCLUSIONS

In analyzing the relative abilities of the VTST and the Rayleigh quotient methods to precisely predict the rate of thermally activated barrier crossing processes in condensed media, we have uncovered some unexpected qualifications on the bounding properties of these methods. Our study was motivated by a recent paper of Talkner and Pollak [22], who demonstrated a restricted identity between these two variational approaches. The identity is formulated as follows: if VTST is restricted to planar dividing surfaces and the Rayleigh quotient method is limited to Kramers trial functions, then the two methods are equivalent. Furthermore, based on the ''upper bound property'' of the VTST method, Talkner and Pollak concluded that for this restricted class of trial functions, the Rayleigh quotient provides an upper bound to the rate not only in the strong friction limit but also in the whole friction range. The latter result is not trivial, as it demonstrates a bounding property for a non-Hermitian operator.

In the present paper, we have shown that the above-mentioned derivations of Talkner and Pollak are correct only in the limit of high barriers $\beta E\to\infty$. Outside of this limit, i.e., for moderate and low barriers, the VTST and the Rayleigh quotient methods are, in fact, *not* identical even when the former is restricted to planar dividing surfaces and the latter is limited to Kramers trial functions. Additionally, we have proven the unexpected result that VTST does *not* provide a rigorous upper bound to the exact rate constant, defined as the least nonvanishing eigenvalue of the Fokker–Planck operator. Even more importantly, we confirm that VTST *does* give an upper bound to the standard numerical reactive flux result (based on the same dividing surface),

from which it follows that the reactive flux result also fails to bound the least nonvanishing eigenvalue (except as $\beta E \rightarrow \infty$). We therefore introduced an improved reactive flux expression, which overcomes this drawback. Finally, we have demonstrated that the Rayleigh quotient, which gives a rigorous upper bound to the least nonvanishing eigenvalue in the Smoluchowski limit, also *looses* its bounding property away from this strong friction limit. Yet, we have shown that in spite of the lack of a bounding property as the reduced barrier height βE decreases, the Rayleigh quotient result continues provide a good estimate of the rate. This stands in contrast to the VTST result, whose accuracy deteriorates rapidly as the barrier decreases and the bounding property is lost.

Although we have restricted ourselves in this paper to Ohmic friction, the present analysis can be generalized to cover systems with memory friction. In such a case, introducing a sufficient number of auxiliary variables, one may transform the original non-Markovian process to an equivalent Fokker-Planck dynamics [28,35] and then again use VTST and the Rayleigh quotient method to estimate the rate [22].

Closing this paper we would like to note the power of the Rayleigh quotient method. Contrary to the standard reactive flux formulation underlying VTST, the Rayleigh quotient provides a precise definition of the kinetic rate which involves *no* unknown factor [like c_1 in Eq. (2.14)] and is applicable regardless of whether or not there exist a separation of time scales. As long as the dynamics are dominated by spatial diffusion across the barrier, this method is capable of giving highly accurate results for the least nonvanishing eigenvalue even when the barrier becomes vanishingly low, $\beta E \rightarrow 0$. Indeed, in all the cases considered herein the optimized Rayleigh quotient result was, throughout the spatial diffusion regime, found to be within 0.5% of the exact rate. Additionally, the accuracy of the Rayleigh quotient method which is based on the Kramers trial function as zeroth-order approximation can be *systematically* improved via perturbation theory [11,8,30].

ACKNOWLEDGMENTS

We thank Alexander Berezhkovskii, Eli Pollak, and Peter Talkner for many stimulating discussions and helpful comments on our work. This work was supported by the National Science Foundation under Grant No. CHE-9727361, and S.C.T. acknowledges the National Science Foundation Young Investigator Program and the Dreyfuss Foundation for financial support.

[1] See, e.g., P. M. Morse and H. Feshbach, *Methods of Theoretical Physics* (McGraw-Hill, New York, 1953).
[2] P. W. Langhoff, S. T. Epstein, and M. Karplus, Rev. Mod. Phys. **44**, 602 (1972); A. K. Kerman and S. E. Koonin, Ann. Phys. (Leipzig) **100**, 332 (1976); R. D. Coalson and M. Karplus, J. Chem. Phys. **93**, 3919 (1990); M. Messina, B. C. Garrett, and G. K. Schenter, *ibid.* **100**, 6570 (1994).
[3] H. Risken, *The Fokker-Planck Equation, Methods of Solution and Applications* (Springer, New York, 1989).
[4] P. Hänggi, P. Talkner, and M. Borkovec, Rev. Mod. Phys. **62**, 251 (1990).
[5] For a recent review, see Chem. Phys. **235**, 1 (1998), special issue on dynamical processes in condensed phases, edited by P. Talkner, E. Pollak, and A. M. Berezhkovskii.
[6] H. Kramers, Physica (Utrecht) **7**, 284 (1940).
[7] R. S. Larson and M. D. Kostin, J. Chem. Phys. **69**, 4821 (1978); O. Edholm and O. Leimar, Physica A **98**, 313 (1979); W. Bez and P. Talkner, Phys. Lett. A **82A**, 313 (1981).
[8] A. N. Drozdov and P. Talkner, Phys. Rev. E **54**, 6160 (1996).
[9] R. S. Larson and M. D. Kostin, J. Chem. Phys. **72**, 1392 (1980); **77**, 5017 (1982); H. Dekker, Phys. Lett. **112A**, 197 (1985); Physica A **135**, 80 (1986); A. N. Drozdov, *ibid.* **187**, 329 (1992).
[10] P. Talkner, Ber. Bunsenges. Phys. Chem. **95**, 327 (1991).
[11] P. Talkner, Chem. Phys. **180**, 199 (1994).
[12] R. Zwanzig, J. Stat. Phys. **9**, 215 (1973).
[13] J. C. Keck, Adv. Chem. Phys. **13**, 85 (1967).
[14] K. J. Laidler, *Theories of Chemical Reaction Rates* (McGraw-Hill, New York, 1969).
[15] P. Pechukas, in *Dynamics of Molecular Collisions, Part B*, edited by W. H. Miller (Plenum, New York, 1976), p. 269.
[16] Yu. I. Dakhnovskii and A. A. Ovchinnikov, Phys. Lett. **113A**, 147 (1985); E. Pollak, Chem. Phys. **85**, 865 (1986).
[17] E. Pollak, S. C. Tucker, and B. J. Berne, Phys. Rev. Lett. **65**, 1399 (1990).
[18] E. Pollak, J. Chem. Phys. **93**, 1116 (1990); A. M. Frishman and E. Pollak, *ibid.* **96**, 8877 (1992); , **98**, 9532 (1993); A. M. Frishman, A. M. Berezhkovskii, and E. Pollak, Phys. Rev. E **49**, 1216 (1994).
[19] A. M. Berezhkovskii, E. Pollak, and V. Yu. Zitserman, J. Chem. Phys. **97**, 2422 (1992).
[20] S. C. Tucker, in *New Trends in Kramers' Reaction Rate Theory*, edited by P. Talkner and P. Hänggi (Kluwer Academic, Dordrecht, 1995), p. 5.
[21] E. Pollak, in *Dynamics of Molecules and Chemical Reactions*, edited by R. E. Wyatt and J. Z. H. Zhang (Dekker, New York, 1996), p. 617.
[22] P. Talkner and E. Pollak, Phys. Rev. E **50**, 2646 (1994).
[23] T. Yamamoto, J. Chem. Phys. **33**, 281 (1960); R. Zwanzig, Annu. Rev. Phys. Chem. **16**, 67 (1965); H. D. Kutz, I. Oppenheim, and A. Ben-Reuven, J. Chem. Phys. **61**, 3313 (1974).
[24] D. Chandler, J. Chem. Phys. **68**, 2959 (1978).
[25] D. Borgis and M. Moreau, Mol. Phys. **57**, 33 (1986); D. J. Tannor and D. Kohen, J. Chem. Phys. **100**, 4932 (1994); J. M. Sancho, A. H. Romero, and K. Lindenberg, *ibid.* **109**, 9888 (1998).
[26] M. Borkovec and P. Talkner, J. Chem. Phys. **92**, 5307 (1990).
[27] J. E. Straub, M. Borkovec, and B. J. Berne, J. Chem. Phys. **83**, 3172 (1985); **84**, 1788 (1986); S. C. Tucker, *ibid.* **101**, 2006 (1994); S.K. Reese, S. C. Tucker, and G. K. Schenter, *ibid.* **102**, 104 (1995); C. Dellago, P. G. Bolhuis, D. Chandler, *ibid.* **109**, 6617 (1999).
[28] A. N. Drozdov and P. Talkner, J. Chem. Phys. **109**, 2080 (1998).

[29] W. Nadler and K. Schulten, J. Chem. Phys. **82**, 151 (1985); P. Jung and H. Risken, Z. Phys. B: Condens. Matter **59**, 469 (1985).
[30] A. N. Drozdov and J. J. Brey, J. Chem. Phys. **110**, 7133 (1999).
[31] A. N. Drozdov and P. Talkner, J. Chem. Phys. **105**, 4117 (1996).
[32] A. N. Drozdov and S. Hayashi, Phys. Rev. E **60**, 3804 (1999).
[33] A. N. Drozdov, J. Chem. Phys. **107**, 3505 (1997); A. N. Drozdov and J. J. Brey, Phys. Rev. E **57**, 1284 (1998).
[34] This is also seen from the dependence of $\Gamma_{\mathrm{RQ}}[\omega=0]$ of the friction coefficient γ. With $\gamma\rightarrow 0$ the functional $\Gamma_{\mathrm{RQ}}[\omega=0]$ decreases and becomes even negative for $\gamma<(\beta\langle x^2\rangle)^{-1/2}$. This failure of the Rayleigh quotient method for $\gamma\lesssim\omega_b$ is due to the Kramers trial function ξ. One can readily show that in the limit of vanishing friction, Eq. (3.9) reduces to $\xi=2\theta(\omega v-\omega^2 x)-1$ and thus no longer provides a good approximation to the true eigenfunction $h_1(x,v)$.
[35] E. Guardia, F. Marchesoni, and M. San Miguel, Phys. Lett. **100A**, 15 (1984).